A solitary wave solution of the Maxwell-Dirac equations

1995 J. Phys. A: Math. Gen. 28 5385

(http://iopscience.iop.org/0305-4470/28/18/026)

J. Phys. A: Math. Gen. 28 (1995) 5385–5392. Printed in the UK

A solitary wave solution of the Maxwell–Dirac equations

A Garrett Lisi

Department of Physics, University of California San Diego, La Jolla, CA 92093-0319, USA

Received 13 February 1995

Abstract. We investigate a class of localized stationary numerical solutions to the Maxwell–Dirac system of classical nonlinear field equations in 3+1 dimensions. The solutions are discrete energy eigenstates bound predominantly by the self-produced electric field.

1. Introduction

There are many examples of classical solitary wave solutions to nonlinear field theory equations. Some of these are useful in quantum field theory as a first-order solution to a semiclassical expansion of the quantized field equations [1]. Although these solutions are often relegated to model equations in fewer than three space dimensions [2], we consider the Maxwell–Dirac system of equations in (3+1)-dimensional spacetime, a nonlinear system of PDEs involving twelve real functions of four variables. The general solution of this system is certainly well beyond our grasp, however, we will obtain a class of particular solutions by making simplifying assumptions and utilizing numerical methods.

Before we embark on a search for a localized solution it would be wise to consider on what grounds such a solution is plausible. It is well known that when one considers the Dirac equation with an external 'repulsive' potential the possibility arises to obtain bound-state solutions [3]. This potential produces bound states with discrete energies that rise from the continuum of free negative energy states in the same way that an 'attractive' potential produces lower energy states from those of positive energy. For a great enough 'repulsive' potential we may even obtain bound states of positive energy. This interesting phenomenon goes under the name of 'Klein's paradox' and provides our motivation. In our case the 'repulsive' potential is provided by the charge feeling its own electric field.

2. Field equations

The Maxwell–Dirac equations are obtained from the well known Lagrangian density

$$L = \mathrm{i}\bar{\Psi}\gamma^{\mu}\partial_{\mu}\Psi - \bar{\Psi}\Psi - q\bar{\Psi}\gamma^{\mu}\Psi A_{\mu} - \tfrac{1}{4}F^{\mu\nu}F_{\mu\nu} \tag{2.1}$$

in which the c-number fields are the Dirac spinor Ψ, which can be considered a four-component single-column matrix, and we have $A^{\mu} = (\Phi, \boldsymbol{A})$, $\bar{\Psi} \equiv \Psi^{\dagger}\gamma^{0}$, $F^{\mu\nu} \equiv \partial^{\mu}A^{\nu} - \partial^{\nu}A^{\mu}$, $\partial_{\mu} \equiv \partial/\partial x^{\mu}$, $x^{\mu} = (t, \boldsymbol{x})$, and γ^{μ} are the 4×4 matrices

$$\gamma^{0} \equiv \begin{pmatrix} I & 0 \\ 0 & -I \end{pmatrix} \qquad \boldsymbol{\gamma} \equiv \begin{pmatrix} 0 & \boldsymbol{\sigma} \\ -\boldsymbol{\sigma} & 0 \end{pmatrix}$$

0305-4470/95/185385+08$19.50

in which I is the 2×2 identity matrix and σ represents the Pauli matrices

$$\sigma_x \equiv \begin{pmatrix} 0 & 1 \\ 1 & 0 \end{pmatrix} \qquad \sigma_y \equiv \begin{pmatrix} 0 & -\mathrm{i} \\ \mathrm{i} & 0 \end{pmatrix} \qquad \sigma_z \equiv \begin{pmatrix} 1 & 0 \\ 0 & -1 \end{pmatrix}.$$

The Euler–Lagrange equations applied to (2.1) give the Maxwell–Dirac equations

$$\gamma^\mu(\mathrm{i}\partial_\mu - qA_\mu)\Psi - \Psi = 0 \tag{2.2}$$

$$\partial_\nu F^{\nu\mu} = q\bar{\Psi}\gamma^\mu\Psi\,. \tag{2.3}$$

Throughout we use natural units, in which we have rescaled length, mass and time so that $\hbar = m = c = 1$.

We now begin making assumptions about the solution we wish to look for. We require that A^μ satisfy the Lorentz condition $\partial_\mu A^\mu = 0$ and that Ψ is an energy eigenstate, $\Psi = \psi(x)\mathrm{e}^{-\mathrm{i}Et}$. Equation (2.3) now reduces to Poisson's equation

$$\nabla^2 A^\mu = -j^\mu \tag{2.4}$$

where j^μ is the 4-current

$$j^\mu = q\bar{\psi}\gamma^\mu\psi \tag{2.5}$$

and equation (2.2) can be written as a Hamiltonian eigenvalue equation

$$E\psi = H\psi = \left[\gamma^0\boldsymbol{\gamma}\cdot(-\mathrm{i}\boldsymbol{\nabla} - q\boldsymbol{A}) + \gamma^0 + q\Phi\right]\psi\,. \tag{2.6}$$

We would now like to assume spherical symmetry for our wavefunction, however, we find that the resulting vector potential $\boldsymbol{A}$ has an angular dependence that destroys the symmetry. This gives us two options: we may throw out the magnetic term in the hope that its contribution will be small and solve the resulting one-dimensional spherically symmetric problem, or we may attack the non-spherical problem. We proceed with the former and save the latter for section 5. By removing $\boldsymbol{A}$ we reduce the Maxwell–Dirac system (2.1) to a massless scalar Dirac system

$$L = \mathrm{i}\bar{\Psi}\gamma^\mu\partial_\mu\Psi - \bar{\Psi}\Psi - q\bar{\Psi}\gamma^0\Psi\Phi + \tfrac{1}{2}(\partial_\mu\Phi)(\partial^\mu\Phi)\,. \tag{2.7}$$

Note that, with γ^0 in the coupling term, our massless scalar Dirac system (2.7) is not Lorentz invariant and is therefore only of use in approximating the Maxwell–Dirac system.

The necessity for a spherical charge distribution restricts our wavefunction to four possible configurations corresponding to total angular momentum up or down, $m_z = \pm\frac{1}{2}$, and the quantum number $\kappa = \pm 1$,

$$\kappa = -1 \qquad m_z = \tfrac{1}{2} \qquad \text{for } \psi = \begin{pmatrix} g(r) \\ 0 \\ -\mathrm{i}f(r)\cos\theta \\ -\mathrm{i}f(r)\mathrm{e}^{\mathrm{i}\phi}\sin\theta \end{pmatrix}$$

$$\kappa = 1 \qquad m_z = \tfrac{1}{2} \qquad \text{for } \psi = \begin{pmatrix} g(r)\cos\theta \\ g(r)\mathrm{e}^{\mathrm{i}\phi}\sin\theta \\ -\mathrm{i}f(r) \\ 0 \end{pmatrix} \tag{2.8}$$

$$\kappa = -1 \qquad m_z = -\tfrac{1}{2} \qquad \text{for } \psi = \begin{pmatrix} 0 \\ g(r) \\ -\mathrm{i}f(r)\mathrm{e}^{-\mathrm{i}\phi}\sin\theta \\ \mathrm{i}f(r)\cos\theta \end{pmatrix}$$

$$\kappa = 1 \qquad m_z = -\tfrac{1}{2} \qquad \text{for } \psi = \begin{pmatrix} g(r)\mathrm{e}^{-\mathrm{i}\phi}\sin\theta \\ -g(r)\cos\theta \\ 0 \\ -\mathrm{i}f(r) \end{pmatrix}$$

in spherical coordinates (r, θ, ϕ), where we have chosen to orient the angular momentum along the z-axis. Note that the two $\kappa = -1$ configurations have the same angular dependence as the hydrogen ground state. Equations (2.4)–(2.6), neglecting A, now reduce to the radial equations

$$E\begin{pmatrix} g \\ f \end{pmatrix} = \begin{pmatrix} q\Phi + 1 & -\dfrac{\mathrm{d}}{\mathrm{d}r} + \dfrac{\kappa - 1}{r} \\ \dfrac{\mathrm{d}}{\mathrm{d}r} + \dfrac{\kappa + 1}{r} & q\Phi - 1 \end{pmatrix}\begin{pmatrix} g \\ f \end{pmatrix} \tag{2.9}$$

$$\Phi'' + \frac{2}{r}\Phi' = -q(f^2 + g^2). \tag{2.10}$$

We symmetrize the Hamiltonian in (2.9) by the similarity transformation $F \equiv rf, G \equiv rg$, and further simplify (2.9) and (2.10) by identifying the fine structure constant $\alpha \equiv q^2/4\pi$ and defining the potential $V \equiv q\Phi$, giving us

$$E\begin{pmatrix} G \\ F \end{pmatrix} = \begin{pmatrix} V + 1 & -\dfrac{\mathrm{d}}{\mathrm{d}r} + \dfrac{\kappa}{r} \\ \dfrac{\mathrm{d}}{\mathrm{d}r} + \dfrac{\kappa}{r} & V - 1 \end{pmatrix}\begin{pmatrix} G \\ F \end{pmatrix} \tag{2.11}$$

$$(rV)'' = -\frac{4\pi\alpha}{r}(F^2 + G^2). \tag{2.12}$$

We also restrict our wavefunction by imposing the normalization condition

$$1 = \int \mathrm{d}^3x\, \Psi^\dagger\Psi = 4\pi\int_0^\infty \mathrm{d}r(F^2 + G^2) \tag{2.13}$$

ensuring a total charge of q. Note that m_z does not appear in (2.11)–(2.13); hence, the energy levels are independent of the choice $m_z = \pm\frac{1}{2}$.

3. Solution

We may readily solve our system of ODEs (2.11) and (2.12) by a variety of means, including power series solution [4], Padé series approximation [5] and numerical methods. We choose the latter as it seems the most straightforward path to obtaining a solution.

We discretize equations (2.11) and (2.12) using second-order finite differences to obtain a standard linear symmetric matrix eigenvalue problem for $(G(r), F(r))$ and E coupled nonlinearly to a symmetric matrix inverse problem for rV. We obtain solutions by solving each linear problem independently and iterating to convergence from an initial guess. This technique is similar to Newton's method of solving the nonlinear system but allows for better behaviour in solving the eigenvalue problem at the cost of slower convergence. We use inverse iteration for the eigenvalue problem together with the conjugate gradient method [6] for the matrix inverses. Although more efficient methods are available for the one-dimensional problem [7], we have chosen methods which will work equally well for the case of two independent variables discussed in section 5.

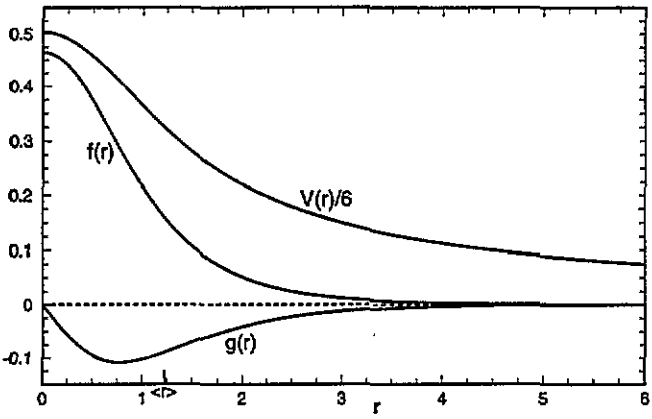

Figure 1. A normalized localized solution to our scalar Dirac system for the choice of $\alpha = 2.7$, $\kappa = 1$ and $n = 0$, showing $f(r)$, $g(r)$ and $V(r)$ scaled down by a factor of six to be fully visible. Note the asymptotic behaviour of $V(r) \simeq \alpha/r$ for large r. The expectation value $\langle r \rangle$ is also shown. All values are in natural units. The one-dimensional mesh was discretized into 200 points for this calculation.

Table 1. Numerical results for our scalar Dirac approximation on a 200 point mesh for several choices of α, n and κ. All values shown are in natural units.

α	n	κ	E	ΔE_M	$\langle r \rangle$	$\mu_z/(qm_z)$
1/137	0	1	$-1 + 9 \times 10^{-6}$	−0.00	572.0	−1.2
0.1	0	1	$-1 + 2 \times 10^{-3}$	−0.00	42.0	−1.2
1.0	0	1	−0.83	−0.00	4.1	−1.1
2.0	0	1	−0.28	−0.05	1.9	−1.0
2.4	0	1	0.09	−0.10	1.5	−0.9
2.7[a]	0	1	0.46	−0.16	1.2	−0.8
3.0	0	1	0.93	−0.24	1.0	−0.7
1/137	1	−1	$-1 + 3 \times 10^{-6}$	−0.00	1710.0	−0.4
2.0	1	−1	−0.75	−0.00	5.4	−0.3
3.4	1	−1	0.06	−0.06	2.0	−0.2
3.8	1	−1	0.89	−0.14	1.2	−0.1
3.0	1	1	−0.68	−0.00	6.2	−1.1
5.0	1	1	0.32	−0.05	2.4	−0.9
5.5	1	1	0.90	−0.10	1.8	−0.8
2.0	2	−1	−0.93	−0.00	18.0	−0.4
5.8	2	−1	0.02	−0.03	3.5	−0.2
6.0	2	−1	0.18	−0.03	3.1	−0.2
6.0	2	1	−0.37	−0.01	6.2	−1.0
6.0	3	1	−0.71	−0.00	13.0	−1.1

[a]Solution shown in figure 1.

Figure 1 shows a solution to our system (2.11)–(2.13) for the choice of $\alpha = 2.7$. We may use the numerical solution to calculate expectation values, such as $\langle r \rangle$ and the strength of the neglected magnetic interaction. Table 1 shows the results for various selections of the parameter α, which completely determines the set of solutions. The energy E as a function of α, κ, and the number of nodes in g, represented by n, is shown in figure 2. We can see from figure 2 and directly from (2.11) that localized solutions are only possible for $-1 < E < 1$. Note that positive energy solutions exist for $\alpha > 2.4$ and that there is a spectrum of large n states of energies near negative one for any choice of α.

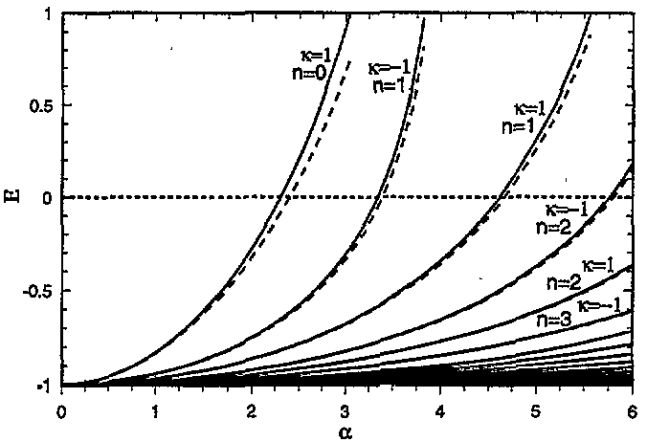

Figure 2. Energy levels as a function of α for our scalar Dirac approximation. The broken curves represent deviations due to the magnetic interaction calculated via the first-order perturbation. All values shown are in natural units.

4. Magnetic interaction perturbation

For the solution to our scalar Dirac equations to be a viable approximate solution to the Maxwell–Dirac equations, we must establish that the inclusion of the magnetic interaction does not significantly alter the solution. We do this properly in section 5 by modelling the larger system (2.4)–(2.6), including the angular dependence. However, we will use perturbation theory with our spherically symmetric solution to determine the approximate energy shift ΔE_M due to the magnetic interaction and find good agreement with the full Maxwell–Dirac case.

The magnetic interaction term in the Hamiltonian density is

$$H_M = -j \cdot A\,. \tag{4.1}$$

We use our solution form (2.8) in equation (2.5) to get the current

$$j = 4q\kappa m_z f(r)g(r)\sin\theta\hat{\phi}\,. \tag{4.2}$$

From this we obtain the vector potential $A = A(r)\sin\theta\hat{\phi}$, in which A is calculated via the Green function integral

$$A(r) = \frac{1}{3}\int_0^\infty \mathrm{d}r_1\, r_1^2 \frac{r_<}{r_>^2} j(r_1) \tag{4.3}$$

where $r_<$ ($r_>$) represents the lesser (greater) of r and r_1. We may now calculate the approximate magnetic energy shift to first order via

$$\begin{aligned}\Delta E_M &\simeq \int \mathrm{d}^3x\, H_M \\ &= -\frac{128}{9}\pi^2\alpha \int_0^\infty \mathrm{d}r\, F(r)G(r)\int_0^\infty \mathrm{d}r_1\, \frac{r_<}{r_>^2}F(r_1)G(r_1)\,.\end{aligned} \tag{4.4}$$

The values obtained for ΔE_M are seen in figure 2 and table 1 and found to be small compared to the binding energy.

We may also use our current (4.2) to calculate the magnetic moment via

$$\mu = \tfrac{1}{2}\int \mathrm{d}^3x(x \times j)$$
$$= 2q\kappa m_z\pi^2 \int_0^\infty \mathrm{d}r\, rF(r)G(r)\hat{z}\,. \tag{4.5}$$

Note in table 1 that we obtain the result $|\mu_z| \simeq \frac{q}{2}$ when we choose $\kappa = 1$.

5. Full Maxwell–Dirac solution

From our calculations in the previous section we expect that the inclusion of the magnetic interaction will result in the emergence of a small non-trivial angular dependence on the θ coordinate. We also expect the solution to maintain its axial symmetry and proceed in cylindrical coordinates (ρ, z, ϕ), assuming a wavefunction of the form

$$\psi = \begin{pmatrix} \psi_1(\rho,z)\mathrm{e}^{\mathrm{i}(m_z-\frac{1}{2})\phi} \\ \psi_2(\rho,z)\mathrm{e}^{\mathrm{i}(m_z+\frac{1}{2})\phi} \\ -\mathrm{i}\psi_3(\rho,z)\mathrm{e}^{\mathrm{i}(m_z-\frac{1}{2})\phi} \\ -\mathrm{i}\psi_4(\rho,z)\mathrm{e}^{\mathrm{i}(m_z+\frac{1}{2})\phi} \end{pmatrix} \tag{5.1}$$

and potentials of the form $\Phi = \frac{1}{q}V(\rho,z)$, $A = \frac{1}{q}A(\rho,z)\hat{\phi}$. Equations (2.4) and (2.5) now reduce to

$$\left(\partial_\rho^2 + \frac{1}{4\rho^2} + \partial_z^2\right)(\sqrt{\rho}V) = -4\pi\alpha\sqrt{\rho}({\psi_1}^2 + {\psi_2}^2 + {\psi_3}^2 + {\psi_4}^2) \tag{5.2}$$

$$\left(\partial_\rho^2 - \frac{3}{4\rho^2} + \partial_z^2\right)(\sqrt{\rho}A) = 8\pi\alpha\sqrt{\rho}(\psi_1\psi_4 - \psi_2\psi_3) \tag{5.3}$$

and the Hamiltonian (2.6) becomes

$$\begin{pmatrix} V+1 & 0 & -\partial_z & -\partial_\rho - \frac{(m_z+\frac{1}{2})}{\rho} + A \\ 0 & V+1 & -\partial_\rho + \frac{(m_z-\frac{1}{2})}{\rho} - A & \partial_z \\ \partial_z & \partial_\rho + \frac{(m_z+\frac{1}{2})}{\rho} - A & V-1 & 0 \\ \partial_\rho - \frac{(m_z-\frac{1}{2})}{\rho} + A & -\partial_z & 0 & V-1 \end{pmatrix}. \tag{5.4}$$

We symmetrize (5.4) by the substitution $\Psi_\alpha \equiv \sqrt{\rho}\psi_\alpha$, giving us

$$E\begin{pmatrix}\Psi_1\\ \Psi_2\\ \Psi_3\\ \Psi_4\end{pmatrix} = \begin{pmatrix} V+1 & 0 & -\partial_z & -\partial_\rho - \frac{m_z}{\rho} + A \\ 0 & V+1 & -\partial_\rho + \frac{m_z}{\rho} - A & \partial_z \\ \partial_z & \partial_\rho + \frac{m_z}{\rho} - A & V-1 & 0 \\ \partial_\rho - \frac{m_z}{\rho} + A & -\partial_z & 0 & V-1 \end{pmatrix}\begin{pmatrix}\Psi_1\\ \Psi_2\\ \Psi_3\\ \Psi_4\end{pmatrix}. \tag{5.5}$$

Note that our wavefunctions in both cases (2.8) and (5.1) are eigenfunctions of the z component of the angular momentum J_z with eigenvalue $m_z = \pm\frac{1}{2}$, where

$$J_z \equiv L_z + \tfrac{1}{2}\Sigma_z \tag{5.6}$$

in which $L \equiv -\mathrm{i}(x \times \nabla)$ and

$$\Sigma \equiv \begin{pmatrix}\sigma & 0\\ 0 & \sigma\end{pmatrix}. \tag{5.7}$$

The full system (5.2)–(5.5) is once again spin-degenerate since the change to $m_z = -m_z'$ produces the same system with the change ($A = -A'$, $\Psi_1 = -\Psi_2'$, $\Psi_2 = \Psi_1'$, $\Psi_3 = \Psi_4'$,

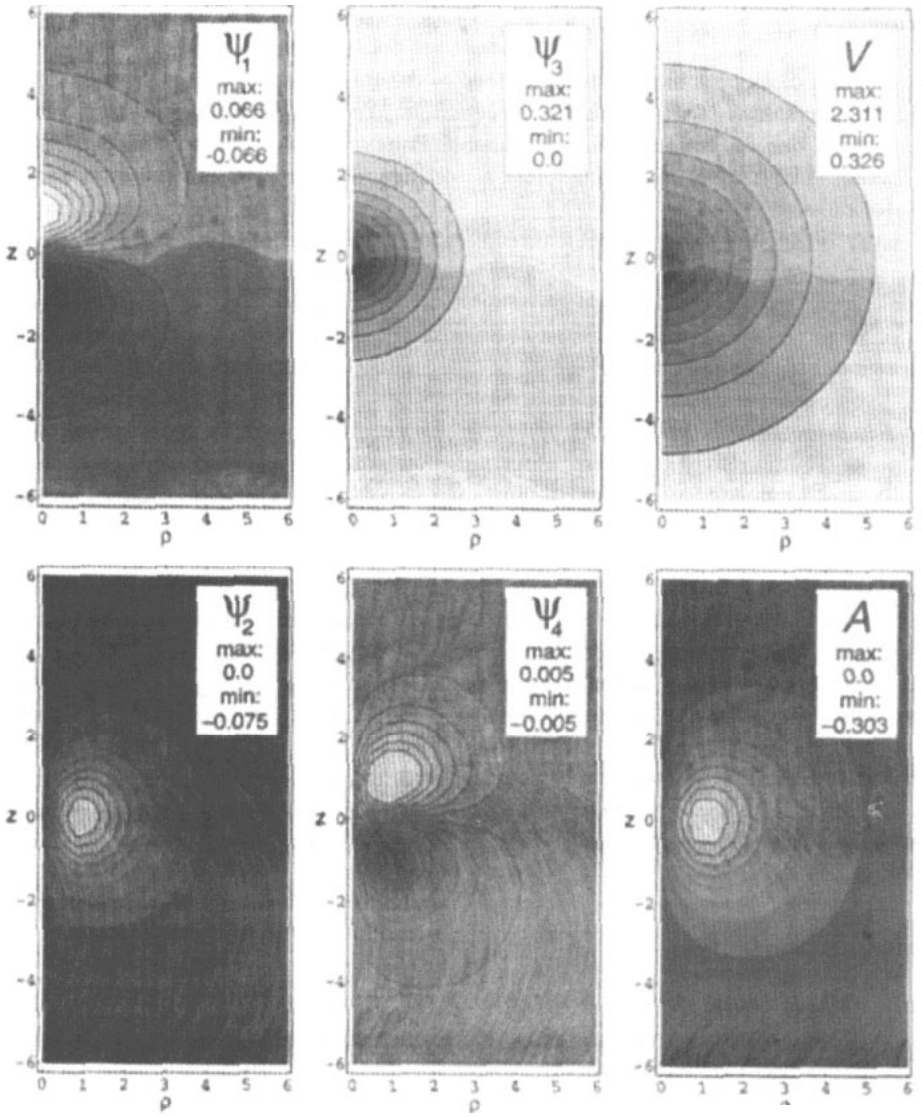

Figure 3. A normalized localized solution to the Maxwell–Dirac system for the choice of $\alpha = 2.7$, showing the four components of the wavefunction $\psi_i(\rho, z)$, the potential $V(\rho, z)$ and the $\hat{\phi}$ component of the vector potential $A(\rho, z)$. The contours go from min (light) to max (dark) and all values are in natural units. The two-dimensional mesh was discretized into $60 \times (2 \times 60 + 1)$ points for this calculation. The energy was calculated as $E_2 = 0.22$, to be compared with that obtained from the one-dimensional approximation, $E + \Delta E_M = 0.30$.

$\Psi_4 = -\Psi_3'$). Although our scalar Dirac wavefunctions (2.9) are eigenfunctions of $K \equiv \gamma^0(\boldsymbol{\Sigma} \cdot \boldsymbol{L} + 1)$ with eigenvalue κ, our solutions of the non-spherically symmetric case will vary slightly from these eigenfunctions.

Figure 3 shows a numerical solution to the full system for the same parameter choice as in figure 1. Note that the angular dependence is virtually indistinguishable from the approximate solution and that the energy agrees reasonably well with the first-order perturbation approximation.

6. Conclusion

We have found a class of solitary wave solutions to the full Maxwell–Dirac equations and good approximate solutions via a scalar Dirac equation. We are, of course, free to translate, rotate and boost our full solution via the suitable Poincaré group operator. In practice, the non-Lorentz-invariant approximate solution is easier to work with and provides better accuracy for most calculations.

The issue of stability has not been directly addressed. The success of our iterative solution method suggests that each solution is stable with regard to slow collapse or expansion. However, we suspect that each solution will be unstable via radiative transitions to states of large negative energy, as is any bound-state solution to the Dirac equation.

Although our solution may be considered of independent interest as the only known exact non-trivial solution to a locally gauge-invariant classical field theory in $3+1$ dimensions, a physical interpretation is not readily apparent. There is always the hope that this sort of soliton-like solution may represent a fundamental particle, however, this conjecture is currently unsubstantiated. As it exists now, we see that our class of solutions to the Maxwell–Dirac system may not be immediately interpreted as representing the leptons. This is clear from the large value of $\langle r \rangle$ and negative value for E for $\alpha = \frac{1}{137}$ as well as from the experimental fact that weak interactions play the starring role in lepton transitions.

Several authors have used similar solutions to construct hadrons from interacting quarks [8, 9], however, these solutions were for systems of nonlinear scalar fields interacting with the Dirac field and the solutions were essentially a result of the nonlinear scalar self-interaction rather than the coupling term. If our solution is to be considered in the construction of hadrons, it will have to be interpreted as a Hartree approximation in the spirit of Witten [10, 11]. Towards this end we note that the substitution of the charge conjugate wavefunction $\Psi_c = \mathrm{i}\gamma^2\Psi^*$ produces the identical system of equations with the sign of the potential and energy spectrum reversed, giving a more sensible bound-state interpretation.

Acknowledgments

I would like to express my appreciation to Roger Dashen and Henry Abarbanel for their encouragement and guidance and to the Hopgood Foundation and the San Diego chapter of the ARCS Foundation for their support.

References

[1] Rajaraman R 1982 *Solitons and Instantons* (Amsterdam: North-Holland)
[2] Das A 1993 *J. Math. Phys.* **34** 3986
[3] Sakurai J J 1967 *Advanced Quantum Mechanics* (Reading, MA: Addison-Wesley)
[4] Rose M E 1961 *Relativistic Electron Theory* (New York: Wiley)
[5] Ditto W L and Pickett T J 1988 *J. Math. Phys.* **29** 1761
[6] Press W 1992 *Numerical Recipes in C* (New York: Cambridge University Press)
[7] Salomonson S and Öster P 1989 *Phys. Rev.* A **40** 5548
[8] Bardeen W L, Drell M S, Weinstein M and Yan T M 1975 *Phys. Rev.* D **11** 1094
[9] Lee T D and Wick G C 1974 *Phys. Rev.* D **9** 2291
[10] Witten E 1979 *Nucl. Phys.* B **160** 57
[11] Poliatzky N 1993 *J. Phys. A: Math. Gen.* **26** 3597